Journal of Peptide Science
J. Peptide Sci. **9**: 753–762 (2003)
Published online in Wiley InterScience (www.interscience.wiley.com). DOI: 10.1002/psc.490

JOURNAL OF PEPTIDE SCIENCE

Three Complete Turns of a 3_{10}-Helix at Atomic Resolution: The Crystal Structure of Z-(Aib)$_{11}$-O*t*Bu‡

RENATE GESSMANN,[a]* HANS BRÜCKNER[b] and KYRIACOS PETRATOS[a]

[a] Institute of Molecular Biology and Biotechnology (IMBB), FORTH, PO Box 1527, 71110 Heraklion, Greece
[b] Interdisciplinary Research Center, Department of Food Sciences, Justus-Liebig-University of Giessen, Heinrich-Buff-Ring 26, 35392 Giessen, Germany

Received 13 February 2003
Revised 19 March 2003
Accepted 20 March 2003

Abstract: The crystal structure of the synthetic protected oligopeptide Z-(Aib)$_{11}$-O*t*Bu was determined by x-ray crystallography. The undecapeptide folds in a regular 3_{10}-helix with nine consecutive $4 \rightarrow 1$ hydrogen bonds. At present, this is the largest available structure of a homopeptide (including homopeptides consisting of standard amino acids) and also the longest observed regular 3_{10}-helix at atomic resolution. Z-(Aib)$_{11}$-O*t*Bu crystallizes readily from hot ethanol–water mixture and is one of the crystals in which no solvent molecule is co-crystallized. In the crystal head-to-tail hydrogen bonded columns are formed in the [$\bar{1}$ 0 $\bar{1}$] direction. Each helical column is surrounded by six others, whereby two are packed in parallel and four in antiparallel fashion. Helical columns are packed via apolar crystal contacts. The crystal structure of Z-(Aib)$_{11}$-O*t*Bu is compared with the crystal structures of Z-(Aib)$_{10}$-O*t*Bu and Z-(Aib)$_9$-O*t*Bu. The similarities and differences are analysed.

Keywords: α-aminoisobutyric acid; 3_{10}-helix; Cα-disubstituted amino acid; undecapeptide

INTRODUCTION

The conformational space available to Aib-residues is severely restricted by the second methyl group attached to the Cα atom. It comprises the left and right handed helical region of the Ramachandran plot and only in a few cases was semi-extended conformation for a *C*-terminal Aib residue observed [1–4]. Aib residues are known as strong helix formers in peptides, favouring α- or 3_{10}-helices. Incorporation of Aib residues in peptides built of conventional residues initiates or stabilizes helical conformation of the whole peptide [5,6]. Helical conformation is a prerequisite for the formation of pores by self-association of naturally occurring peptides rich in Aib-residues (e.g. peptaibols) in lipid bilayer membranes [7,8]. The crystal structures known to date of all homopeptides with more than 4 Aib residues show a clear preference for left and right handed 3_{10}-helices. This is confirmed by ^{1}H-NMR and infrared absorption experiments [9], which have been performed in the low polarity solvent deuteriochloroform ($\varepsilon = 4.9$). The results suggest 3_{10}-helical structure for the Z-(Aib)$_n$-O*t*Bu ($n = 5$–11) homopeptides. All crystal structures of Aib homopeptides [1,2,10–17] show the following common properties: centrosymmetric space group, regular 3_{10}-helices with the maximum number of hydrogen bonds also involving the *N*-terminal protecting group, a reversal of the helical sense in the *C*-terminal residue, head-to-tail hydrogen-bonded columns. In most cases, these columns pack in one direction in antiparallel fashion, and

Abbreviations: Z, benzyloxycarbonyl; O*t*Bu, *tert* butoxy; Aib, α-aminoisobutyric acid; r.m.s., root-mean-square.

* Correspondence to: Dr Renate Gessmann, Institute of Molecular Biology and Biotechnology (IMBB), FORTH, PO Box 1527, 71110 Heraklion, Greece; e-mail: rege777@yahoo.com
‡ Presented at Peptaibols, October 2002, Jena, Germany.

in parallel fashion in the other direction. These parallel columns are often hydrogen-bonded via solvent molecules.

Long stretches of 3_{10}-helices have been considered to be unlikely for several years, because in polypeptides containing Cα-monosubstituted amino acids the geometry of the hydrogen bonds and the steric hindrance of the side chains is less favourable than in α-helices [18,19]; only the additional hydrogen bond per helix makes a 3_{10}-helix energetically more favourable. This is the reason that in a survey [20] of 11 096 residues of proteins only 3.4% are involved in 3_{10}-helices, which are mostly irregularly folded. There are exceptions, e.g. the leucine-rich repeat variant [21] contains seven 3_{10}-helices of a length of 5–9 residues each, with an overall occurrence of 20%. On the other hand, regular 3_{10}-helices with more than two turns seem to occur only in the synthetic Aib-peptides.

MATERIALS AND METHODS

Peptide Synthesis and Characterization

The segments required for the synthesis of the title compound were synthesized via the oxazolone route described previously [22,23]. The segment coupling reported here for the synthesis of the undecapeptide is different from the stepwise procedure [9]. The protected title compound was obtained by reaction of Z-Aib$_{10}$-Ox (Ox refers to the oxazolone formed from the *C*-terminal Aib of the Z-protected peptide acid on reaction with acetic anhydride) with H-Aib-O*t*Bu (5 equivalents) in a mixture of *n*-butyl acetate and 1,1,2,2-tetrachloroethane (9 : 1, v/v) at 100 °C for 36 h. The solvents were removed *in vacuo*, dichloromethane was added and the organic phase was washed successively (3×) with $KHSO_4$ (5%), $KHCO_3$ (5%) and water. The organic phase was dried over Na_2SO_4 and evaporated to dryness. Then the remaining residue was crystallized from a mixture of methanol and chloroform by addition of *n*-hexane. Yield 82%, m.p. 264 °C; R_F 0.28 (mobile phase, ethyl acetate; Kieselgel 60 F_{254}, plate 20 × 20 cm, film thickness 0.25 mm, Merck product no. 105715; spraying with water or chlorine/TDM reagent); electrospray ionization mass spectrum *m/z* 1167.0 $(M + Na)^+$ and a regular series of acylium fragment ions differing by 85.1 mass units (Aib-H_2O) ranging from *m/z* 305.5 (b_2) to *m/z* 1071.3 (b_{11}).

X-Ray Diffraction Analysis

Colourless single crystals were grown from a hot ethanol–water mixture (90 : 10). Two crystal forms were found. The first form was observed in large (1 × 1 × 1 mm) not single crystals with anomalous surfaces. The second form was observed in several small prisms (0.2 × 0.1 × 0.04 mm), which resemble diamonds, because of their cut apices. X-ray diffraction data were collected on an automated Enraf-Nonius CAD-4 [24] diffractometer with graphite monochromated, Ni-filtered CuKα radiation. The unit cell parameters were obtained by least-squares fitting using the angular parameters of 25 reflections ($9^\circ < \theta < 21^\circ$). During data collection, five reflections were monitored every 60 min, in order to check the stability of the crystal and the electronics of the detecting system. The observed intensities varied within 2%. The intensities of all reflections were corrected for this variation as well as for Lorentz and polarization factors (Xtal programs: DIFDAT, SORTRF, ADDREF [25]) and also for absorption by the analytical method applied by ABSOR. The crystal data are listed in Table 1. Initial data collection of the outermost shell ($\Theta = 60^\circ$–65°) was halted after 37 reflections (or 3% completeness), because the ratio of intensity to background was considered to be too low. The structure was solved by direct methods using the GENTAN suite of Xtal. The structure solution revealed 64 out of 81 non-hydrogen atom positions. The remaining atoms were detected by difference Fourier techniques. Anisotropic temperature factor refinement of F^2 was carried out with SHELXL97 against all reflections [26]. *R*-factors based on F^2 are statistically about twice as large as those based on *F*, and *R*-factors based on all data will be even larger [26]. All hydrogen atoms were placed in geometrically calculated positions and the riding model approach was used. For one hydrogen atom the temperature factor was set to 1.5 times the equivalent isotropic one of the atom on which it is riding (a methylated C of O*t*Bu) owing to the unusually high value resulting from refinement. 44 reflections with $\Delta F^2 > 3.2$ were excluded in the last stage of the refinement. In a final difference Fourier map no electron density above 0.4 e/Å^3 or below −0.45 e/Å^3 was found.

CCDC 204587 contains the supplementary crystallographic data for this paper. These data can be obtained free of charge via www.ccdc.cam.ac.uk/conts/retrieving.html (or from the CCDC, 12 Union Road, Cambridge

Table 1 Crystallographic Data for Z-(Aib)$_{11}$-O*t*Bu

Molecular formula	$C_{56}H_{93}N_{11}O_{14}$
Formula weight	1141.41
Crystallization solvent	Ethanol/water
Crystal system	Monoclinic
Space group	$P2_1/c$
a (Å)	16.92(2)
b (Å)	17.46(2)
c (Å)	25.90(3)
β (°)	117.71(5)
Volume (Å^3)	6681(12)
Z (molecules/unit cell)	4
Density (calc.)(g/cm^3)	1.138
Matthew's coefficient	1.463 Å^3/Dalton
Collected reflections	12463
Independent reflections	9958
R(int)	0.029
Θ min/resolution min	2.99°/29.5 Å
Θ max/resolution max	64.7°/0.85 Å
Completeness $\Theta = 2.99 - 60°$	99.55
No. of refined parameters	823
R/wR2 of all reflections	0.271/0.349
No. of refl. $F^2 > 2\sigma(F^2)$	3492
R/wR2 of refl. $F^2 > 2\sigma(F^2)$	0.108/0.256
Goodness of fit	0.919
Average B-factors	
All atoms	13.05 Å^2
Non-hydrogens	6.67 Å^2

CB2 1EZ, UK; fax: +44 1223 336033; e-mail: deposit@ccdc.cam.ac.uk).

RESULTS

Molecular Structure of Z-(Aib)$_{11}$-O*t*Bu

A perspective view of the molecule, based on the experimentally determined coordinates and thermal parameters is shown in Figures 1 and 2, using the ORTEP [27,28] computer program. Aib residues and both protecting groups consist only of achiral atoms, a fact that results in a centrosymmetric space group and the presence of both left and right handed helices in the unit cell. When there was a choice, the right handed helix was chosen for the tables and figures. The backbone torsion angles [29] are listed in Table 2. The overall folding of the undecapeptide is consistent with a regular 3_{10}-helix built of nine consecutive β-turns of type III [30]. The average torsion angles for the right handed conformation are: $<\phi>= -53° \pm 4°$, $<\psi>= -27° \pm 4°$ and $<\omega>= 179° \pm 3°$, which are in good agreement with comparable structures [2,16]. There are nine intramolecular hydrogen bonds of the type $4 \rightarrow 1$, one of them between the carbonyl group of the *N*-terminal protecting group and the amino group of Aib3. The hydrogen bonding parameters are listed in Table 3 and are in good agreement with comparable structures [2,16] and comparable to the observed values for 3_{10}-helices in globular proteins [31].

The valency geometry around the Cα is asymmetric for all Aib residues, a feature proved by theoretical and experimental studies in 3_{10}-helices [32]. Only one exception was found, so far without any clear explanation [33]. If one designates as CL the atom in Aib that occupies the same position as Cβ in L-amino acids and as CR the atom that occupies the same position as the Cα-hydrogen, in the right handed conformation the bond angles N-Cα-CL

Table 2 Conformation Angles (°) of Z-(Aib)$_{11}$-O*t*Bu for the Right Handed Conformation

Residue	Φ	ψ	ω
Aib1	−59(1)	−25(1)	179(1)
Aib2	−49(1)	−35(1)	−178(1)
Aib3	−56(1)	−26(1)	−179(1)
Aib4	−56(1)	−22(1)	176(1)
Aib5	−48(1)	−31(1)	−179(.7)
Aib6	−52(1)	−28(1)	180(.6)
Aib7	−53(1)	−26(1)	179(.6)
Aib8	−54(1)	−21(1)	175(.7)
Aib9	−50(1)	−27(1)	−179(.7)
Aib10	−57(1)	−27(1)	173(.7)
Aib11	55(1)	50(1)	177(.8)

Table 3 Parameters of the Hydrogen Bonds (Å, °)

Donor	Acceptor	N···O	H···O	N–H···O	C–O···H
Intramolecular					
N3	OZ	3.056(9)	2.22	163	128
N4	O1	2.890(9)	2.06	162	128
N5	O2	3.085(10)	2.24	167	127
N6	O3	3.011(9)	2.16	170	132
N7	O4	2.895(9)	2.05	166	129
N8	O5	3.007(9)	2.16	166	128
N9	O6	2.992(9)	2.14	169	129
N10	O7	2.996(9)	2.14	173	130
N11	O8	2.968(10)	2.15	159	127
Intermolecular $x,y,z \rightarrow x-1,y,z-1$					
N1	O10	2.806(10)	1.95	175	135

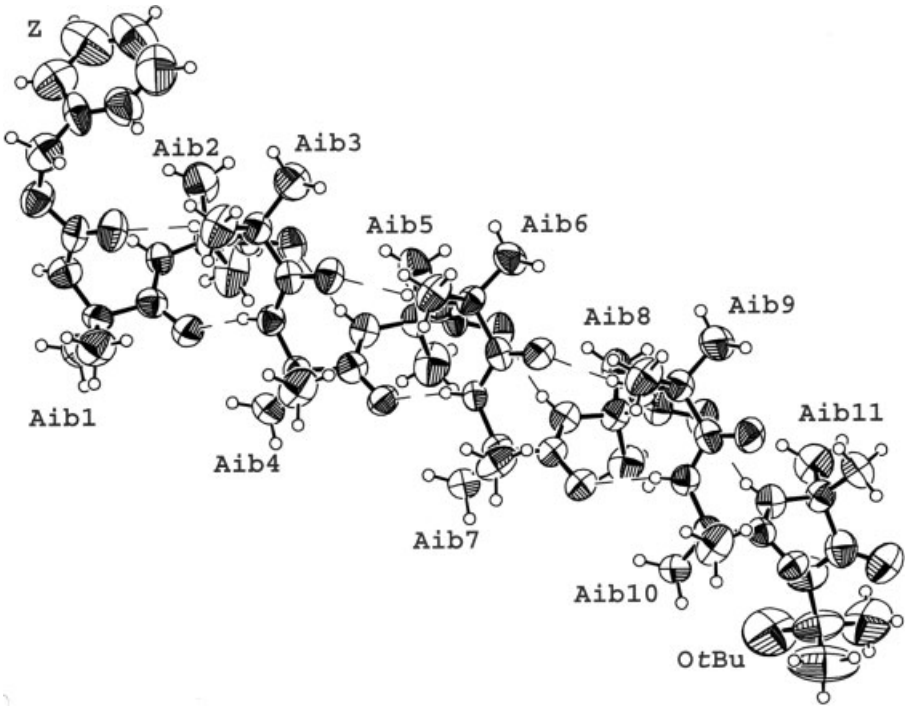

Figure 1 Perspective drawing of the molecular structure of Z-(Aib)$_{11}$-O*t*Bu in the right handed helical conformation using the program ORTEP-III [25,26], contoured at 50% probability. Intramolecular hydrogen bonds are indicated by broken lines.

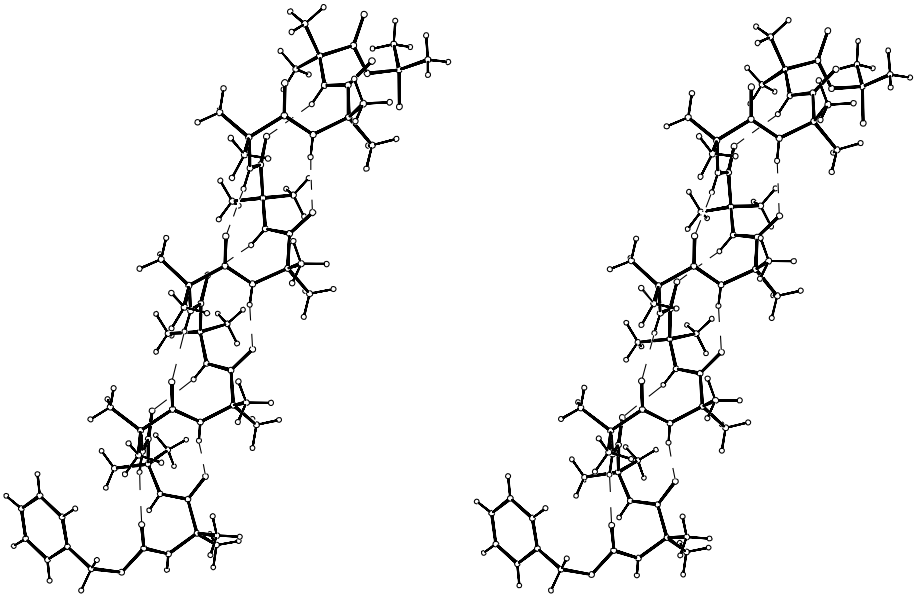

Figure 2 Stereo view of one right handed molecule of Z-(Aib)$_{11}$-O*t*Bu. Intramolecular hydrogen bonds are indicated by broken lines.

and C-Cα-CL in all but one case are smaller (Table 4) than the tetrahedral value (109.45°) and the angles N-Cα-CR and C-Cα-CR are in most cases greater (Aib1-Aib10). The average values are 107.2(7)° for N-Cα-CL, 107.1(8)° C-Cα-CL, 110.6(8)° for N-Cα-CR and 109.3(7)° for C-Cα-CR. The opposite asymmetry is found for the last residues and the left handed helices. Even if the asymmetry for some residues

Table 4 Bond Angles (°) Defining the Valency Geometry Around the Cα-atoms

Residue	N-Cα-CL	C-Cα-CL	N-Cα-CR	C-Cα-CR
Aib1	106.6(7)	107.1(8)	110.0(8)	111.1(8)
Aib2	109.2(7)	107.9(9)	111.3(9)	106.6(6)
Aib3	106.7(7)	105.7(8)	112.2(8)	109.1(7)
Aib4	107.6(6)	107.4(8)	109.9(7)	109.0(7)
Aib5	110.2(9)	106.5(6)	108.4(7)	110.5(9)
Aib6	106.5(6)	105.7(7)	112.1(7)	109.4(6)
Aib7	105.8(6)	108.1(7)	109.6(6)	109.6(6)
Aib8	107.8(6)	108.7(8)	109.4(8)	108.5(6)
Aib9	105.1(7)	107.0(8)	110.8(8)	109.2(7)
Aib10	106.8(6)	107.0(8)	111.4(8)	109.8(7)
Aib11	110.8(7)	110.8(7)	108.0(7)	106.2(8)

is not so pronounced as in other 3_{10}-helices, the behaviour is still a typical finding of Aib containing oligopeptides.

Crystal Packing of Z-(Aib)$_{11}$-O*t*Bu

In the crystal, the peptides are head-to-tail hydrogen bonded along the [$\bar{1}$ 0 $\bar{1}$]-direction, with a remarkable linear and short hydrogen bond (Table 3 and Figure 3). Each of these infinitely long helical columns is surrounded by six others (Figure 4), without any additional hydrogen bond and packed by van der Waals interactions. In the [0 1 0] direction, columns of the alternating handedness are packed in an antiparallel way, building waved layers along the b-axis. In the direction perpendicular to the b-axis these layers are packed via apolar crystal contacts with the neighbouring layers in such a way that left and right handed columns alternate in a parallel way. This results in two parallel and four antiparallel surrounding columns for each helix, whereby two have the same handedness and four the opposite one.

Both protecting groups point outwards from the well packed helix, allowing a larger distance between the helical columns. The program PLATON [34] with the option SOLV or CAVITY detects voids in the structure of 44 and 41 Å^3. These voids are big enough to host a hydrogen-bonded water molecule. In the apolar molecular interface between the helical columns, no hydrogen bonds are possible between a water molecule and any other geometrically available partner. Moreover, the voids are too small for a not hydrogen-bonded water molecule.

Comparison of the Crystal Structures of Z-(Aib)$_9$-O*t*Bu, Z-(Aib)$_{10}$-O*t*Bu and Z-(Aib)$_{11}$-O*t*Bu

Comparisons have been carried out of the very closely related Z-(Aib)$_9$-O*t*Bu, Z-(Aib)$_{10}$-O*t*Bu [2,17] and of the title compound but not of these three structures and *p*-BrBz-(Aib)$_{10}$-O*t*Bu [16]. The heavier Br-atom in the protecting group of the latter compound provides an easier solution for the x-ray data but changes the conformation of the whole molecule as well as the arrangement of the molecules in the crystal [17]. Least-square superpositions were performed of Z-(Aib)$_{9-11}$-O*t*Bu, including the non-hydrogen atoms (starting from the carbonyl of the Z protecting group up to the carbonyl of the last Aib residue) with the program LSQ [35]. Both protecting groups were excluded, due to their variable conformation — which depends on the crystal environment — as shown in Figure 5 [36]. The r.m.s.-deviation values of the least-square superpositions are listed in Table 5. The values obtained were very small. The overall folding is identical and the structures differ mostly at the *C*-terminal region. Nevertheless, the following differences between these three peptides can be highlighted.

(1) While the title compound crystallized within minutes by cooling the hot ethanol–water mixture to room temperature, Aib10 and Aib9 were crystallized from a methanol–water mixture. Aib10 crystals appeared a few weeks later, and the only Aib9 crystal available was detected several years later. In contrast to the title compound, in both other cases solvent molecules (methanol and water) were co-crystallized.
(2) Aib9 has two molecules in the asymmetric unit, one of them is disordered, while both other peptides have only one, not disordered, molecule in the asymmetric unit.

Table 5 Least-square Superposition of Aib$_{9,10,11}$ Homopeptides, Fitted C=O (Z) → C=O (*C*-terminal Aib)

Fit	r.m.s. deviation		At atom
	Average	Maximum	
10 → 11	0.671	2.784	C10A
9 mol A → 11	0.601	1.894	C9L
9 mol B → 11	0.554	1.639	C9R

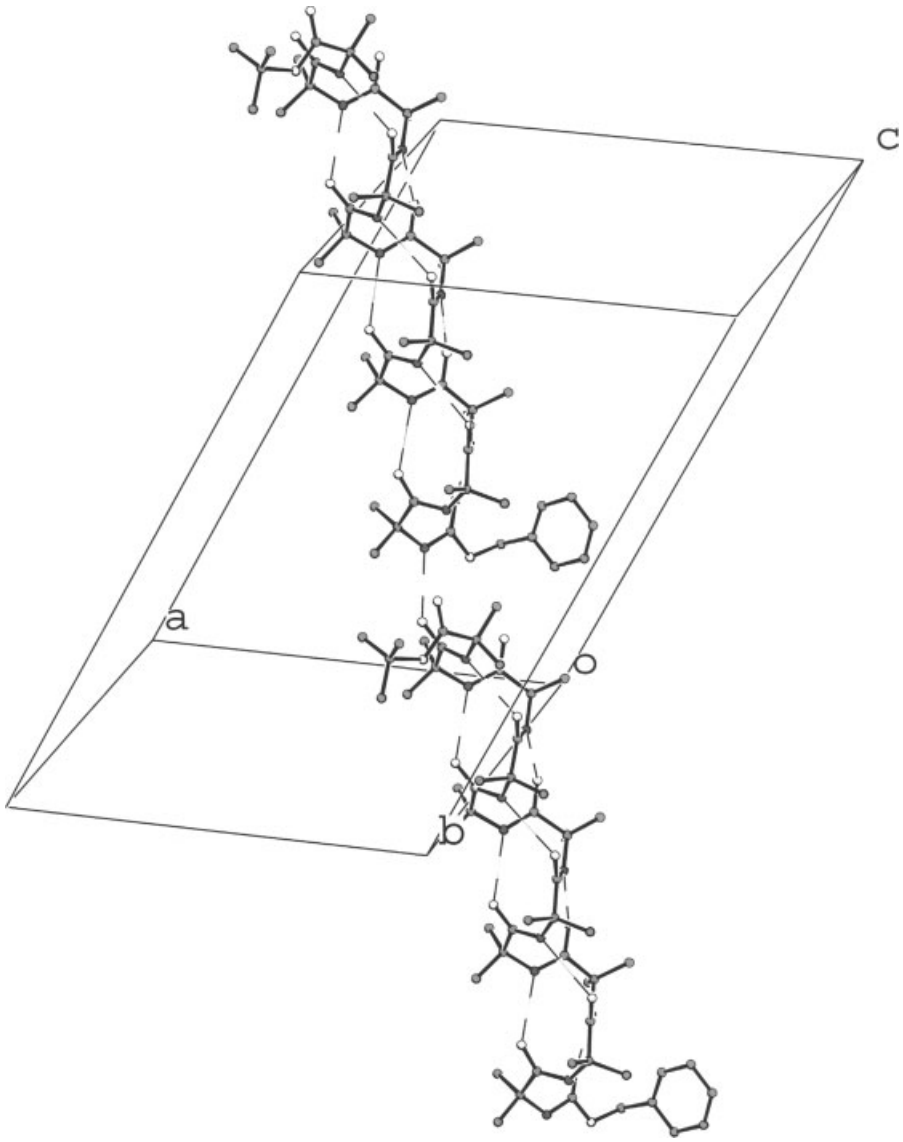

Figure 3 Crystal packing of Z-(Aib)$_{11}$-O*t*Bu. Two molecules that are connected by a hydrogen bond in [$\bar{1}$ 0 $\bar{1}$]-direction are shown.

(3) In the case of Aib9, the head-to-tail infinitely long helical columns consist of alternating molecules A and B with different handedness. In the crystal of Aib10 the columns are formed by molecules of different handedness and, in the case of Aib11 they consist of molecules with the same handedness.
(4) The mode of the crystal packing of the two parallel surrounding columns also differs. In the case of Aib9 and Aib11, parallel columns are packed by apolar crystal contacts, while in the case of Aib10, parallel columns are hydrogen bonded via a water molecule.

The program HELANAL [37] was employed in order to analyse the helical parameters, which are listed in Table 6. Interestingly, the average helical twist increases with chain length and for Z-(Aib)$_{11}$-O*t*Bu is only 2.3° away from the ideal value for a 3_{10}-helix (120°). Also the average number of residues per turn for Z-(Aib)$_{11}$-O*t*Bu is very close to the ideal value of 3 and is lower than for the three other helices. These results demonstrate that the helix of the title compound is more tightly wound than in the remaining helices. Values close to an ideal 3_{10}-helix have been reported also for *p*BrBz-(Aib)$_8$-O*t*Bu [15]. Both *p*BrBz-(Aib)$_8$-O*t*Bu and the

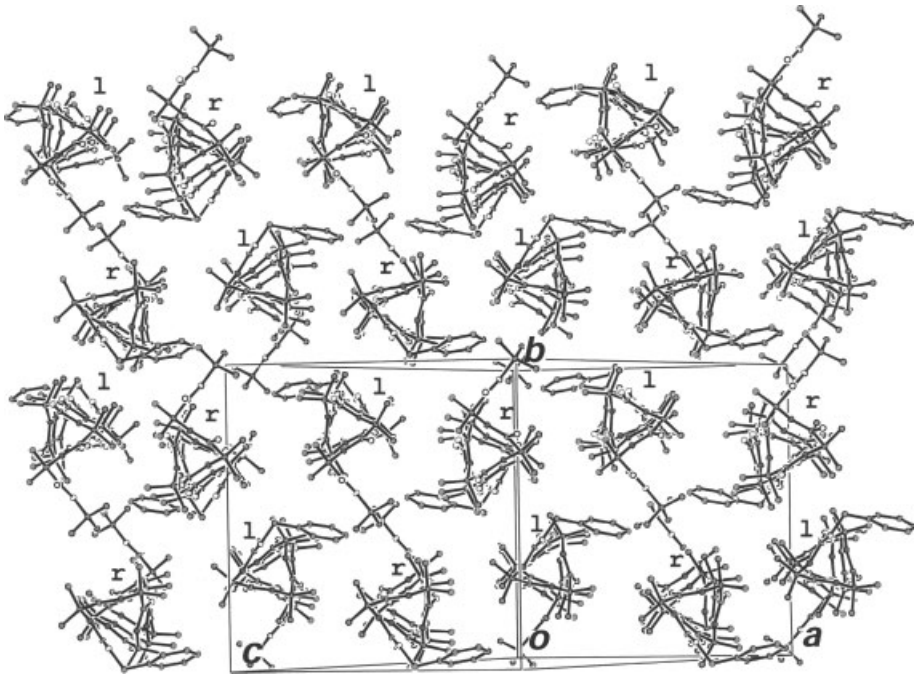

Figure 4 Crystal packing of Z-(Aib)$_{11}$-O*t*Bu viewed down the helical axis of the infinitely long helical columns. The triangle formed by the almost ideal 3_{10}-helix is clearly visible. r and l, resp., denote the handedness of the helix, r right handed, l left handed. The columns in the top and in the third horizontal layer point with the *C*-termini to the viewer, the columns in the second and fourth layer with the *N*-termini.

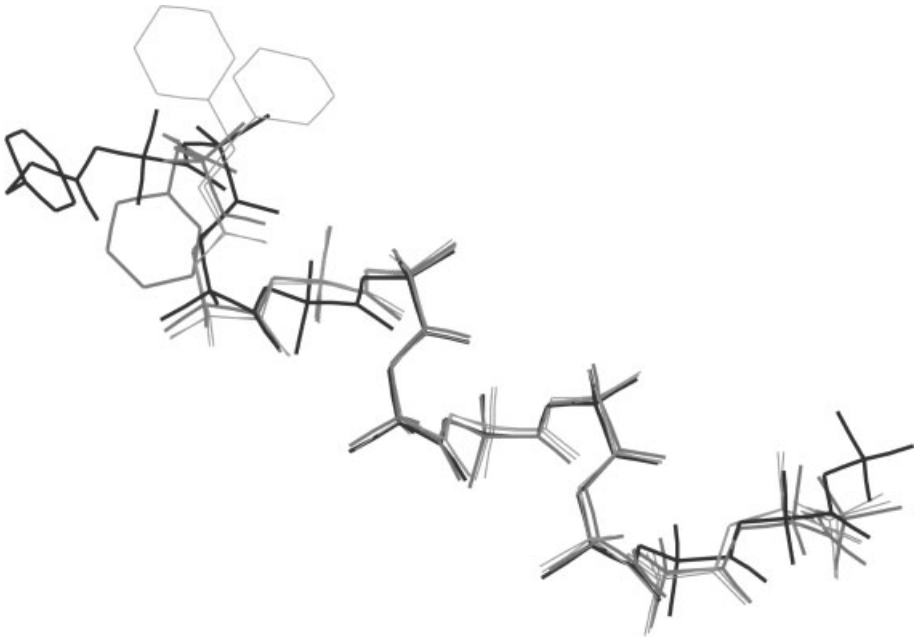

Figure 5 Least-square superposition of the molecular structures of Z-(Aib)$_n$-O*t*Bu with $n = 11$ shown in black, $n = 10$ in dark grey and the two molecules of $n = 9$ in light grey with thin lines.

Table 6 Helical Parameters for Z-$(Aib)_9$-O*t*Bu, Z-$(Aib)_{10}$-O*t*Bu and Z-$(Aib)_{11}$-O*t*Bu. The parameters are derived from helices comprising the *C*-terminal moiety of the Z-protecting group and all Aib residues

Helix	Average number of residues/ turn	Average rise per residue [Å]	Average helical twist per residue [°]
Z-$(Aib)_9$-O*t*Bu mol A	3.21(10)	1.94(05)	112.27(3.6)
Z-$(Aib)_9$-O*t*Bu mol B	3.20(07)	1.93(05)	112.64(2.6)
Z-$(Aib)_{10}$-O*t*Bu	3.17(08)	1.98(07)	113.46(2.8)
Z-$(Aib)_{11}$-O*t*Bu	3.06(07)	1.98(04)	117.73(2.5)

title compound possess full turns of 3_{10}-helix, which seems to stabilize the internal structure. This is confirmed by thin layer chromatography experiments: in butyl acetate–methanol and ethyl acetate the homopeptides with full turns ($n = 5$, 8, 11) show relatively higher retention factor R_F-values compared with the homopeptides, which have one residue more or less [23]. In agreement, their melting point also shows higher values than the neighbouring peptides.

DISCUSSION

In all crystallographic studies of Aib-containing peptides two types of helices are formed by Aib containing peptides: the α-helix with hydrogen bonds of type $5\rightarrow1$ and the more tightly wound 3_{10}-helix with hydrogen bonds of type $4\rightarrow1$. The consensus is that smaller peptides with a high content of Aib prefer the 3_{10}-helical conformation [19,38]. Furthermore, by enlarging the length of the peptide — depending on the composition and other parameters — a transition length is reached, whereby the peptide adopts an α-helical conformation. *Inter alia*, the dielectric constant of the solvent influences the type of the helix of the peptides by changing the Coulombic interactions. In model calculations [39] with solvents of low dielectric constant, the helix formed is predominantly 3_{10} and in high dielectric environment it is α-helical. There are hints that confirm the latter finding in the crystal structures of the same peptide co-crystallized with different solvents [4,40].

Peptides consisting of merely Aib residues are excellent models for calculations of a probable transition between 3_{10}- and α-helix because of their simplicity. Several model calculations for the type of helix (3_{10} or α) of Aib-homopeptides have been performed [39,41–43], which also include the structure of the title compound. Most of the calculations were carried out *in vacuo* and in a higher dielectric constant environment. Interestingly, all predict Aib_{11} to be clearly α-helical with the only exception being the most recent publication. Improta *et al.* [43] concluded that, the preference of 'Aib infinite homopeptides' *in vacuo* for 3_{10}-helices is mainly due to the severe distortion of a hypothetical α-helix induced by methyl–methyl interresidue repulsions. Zhang and Hermans [44] concluded in their molecular dynamics study for Aib_{10} no clear helical preference in water ($\varepsilon = 78$) but 3_{10}-helical preference *in vacuo* ($\varepsilon = 1$), while Smythe *et al.* [45,46] concluded in free energy surface calculations for the helical transition for Aib_{10} clearly α-helical preference *in vacuo* and different other solvents. Other authors [39,41] reported the improved packing of 3_{10}-helices in a hypothetical crystal. Naturally, the environment *in vacuo* or in solution, especially at a low concentration of peptide, differs from the environment in the crystal, in which intermolecular interactions between the peptides become more important and may actually dominate.

Attempts are in progress to crystallize the title compound with different solvents in place of that described in the present work, whereby the crystallization resulted in a crystal environment without any solvent molecule. Hopefully, a solvent with high dielectric constant will — by co-crystallization — change the dielectric environment in the crystal and may force the structure away from the regular 3_{10}-helix. In addition, based on the above results, one can conclude that peptides with not complete turns of 3_{10}-helices would be better candidates for forming a structure different from a regular 3_{10}-helix.

REFERENCES

1. Di Blasio B, Pavone V, Pedone C, Benedetti E, Moretto V, Crisma M, Toniolo C. Crystal-state conformation of homo-oligomers of α-aminoisobutyric acid: molecular and crystal structure of *p*BrBz-$(Aib)_6$-OMe. *Struct. Chem.* 1991; **2**: 523–537.
2. Geßmann R, Brückner H, Kokkinidis M. Structure of Z-$(Aib)_9$-OBut. *Acta Crystallogr.* 1998; **B54**: 300–307.
3. Karle IL, Flippen-Anderson JL, Sukumar M, Balaram P. Aqueous channels within apolar peptide aggregates: Solvated helix of the α-aminoisobutyric

acid (Aib)-containing peptide Boc-(Aib-Ala-Leu)$_3$-Aib-OMe•H_2O•CH_3OH in crystals. *Proc. Natl Acad. Sci. USA* 1988; **85**: 299–303.
4. Karle IL, Flippen-Anderson JL, Uma K, Balaram P. Helix aggregation in peptide crystals: occurrence of either all parallel or antiparallel packing motifs for α-helices in polymorphs of Boc-Aib-Ala-Leu-Ala-Leu-Aib-Leu-Ala-Leu-Aib-OMe. *Biopolymers* 1990; **29**: 1835–1845.
5. Karle IL, Flippen-Anderson JL, Uma K, Balaram H, Balaram P. Peptide design: Influence of a guest Aib-Pro segment on the stereochemistry of an oligo-Val sequence — solution conformations and crystal structure of Boc-(Val)$_2$-Aib-Pro-(Val)$_3$-OMe. *Biopolymers* 1990; **29**: 1433–1442.
6. Gurunath R, Balaram P. Incorporation of a potentially helix breaking D-Phe-Pro sequence into the center of a right handed 16 residue peptide helix. *Biochem. Biophys. Res. Commun.* 1994; **202**: 241–245.
7. Sansom MSP. Structure and function of channel-forming peptaibols. *Quart. Rev. Biophys.* 1993; **26**: 365–421.
8. Chugh JK, Brückner H, Wallace BA. Model for a helical bundle channel based on the high-resolution crystal structure of trichotoxin_A50E. *Biochemistry* 2002; **41**: 12 934–12 941.
9. Toniolo C, Bonora GM, Barone V, Bavoso A, Benedetti E, di Blasio B, Grimaldi P, Lelj F, Pavone V, Pedone C. Conformation of pleionomers of α-aminoisobutyric acid. *Macromolecules* 1985; **18**: 895–902.
10. Shamala N, Nagaraj R, Balaram P. The 3_{10}-helical conformation of a pentapeptide containing α-aminoisobutyric acid (Aib): X-ray structure of Tos-(Aib)$_5$-OMe. *J. Chem. Soc. Chem. Commun.* 1978; 996–997.
11. Benedetti E, Bavoso A, di Blasio B, Pavone V, Pedone C, Crisma M, Bonora GM, Toniolo C. Solid-state and solution conformation of homo oligo(α-aminoisobutyric acids) from tripeptide to pentapeptide: evidence for a 3_{10} helix. *J. Am. Chem. Soc.* 1982; **104**: 2437–2444.
12. Vlassi M, Brückner H, Kokkinidis M. The crystal structure of the conformationally constrained peptide Z-(Aib)$_6$-OBu^t. *Zeit. Kristallogr.* 1992; **202**: 89–98.
13. Pavone V, di Blasio B, Pedone C, Santini A, Benedetti E, Formaggio F, Crisma M, Toniolo C. Preferred conformation of homo-oligomers of α-aminoisobutyric acid: molecular and crystal structure of Z-(Aib)$_7$-OMe. *Gazz. Chim. Ital.* 1991; **121**: 21–27.
14. Vlassi M, Brückner H, Kokkinidis M. Peptide with built in constraints: Structure of Z-(Aib)$_7$-O*t*Bu. *Acta Crystallogr.* 1993; **B49**: 560–564.
15. Bavoso A, Benedetti E, di Blasio B, Pavone V, Pedone C, Toniolo C, Bonora GM. Long polypeptide 3_{10}-helices at atomic resolution. *Proc. Natl Acad. Sci. USA* 1986; **83**: 1988–1992.
16. Toniolo C, Crisma M, Bonora GM, Benedetti E, di Blasio B, Pavone V, Pedone C, Santini A. Preferred conformation of the terminally blocked (Aib)$_{10}$ homo-oligopeptide: A long regular 3_{10}-helix. *Biopolymers* 1991; **31**: 129–138.
17. Geßmann R. *Kristallstrukturen von Aib-enthaltenden Oligopeptiden*. PhD thesis, Universität Hohenheim, Germany, 1999.
18. Schulz GE, Schirmer RH. In *Principles of Protein Structure*, Cantor CR (ed.). Springer-Verlag: New York, 1979; 69–72.
19. Toniolo C, Benedetti E. The polypeptide 3_{10}-helix. *Trends Biochem. Sci.* 1991; **16**: 351–353.
20. Barlow DJ, Thornton JM. Helix geometry in proteins. *J. Mol. Biol.* 1988; **201**: 601–619.
21. Peters JW, Stowell MHB, Rees DC. A leucine-rich repeat variant with a novel repetitive protein structural motif. *Nature Struct. Biol.* 1996; **3**: 991–994.
22. Leplawy MT, Jones DS, Kenner GW, Sheppard RC, Peptides XI. Synthesis of peptides derived from α-methylalanine. *Tetrahedron* 1960; **11**: 39–51.
23. Brückner H. Oxazolone activation in the synthesis of oligopeptides containing α-methylalanine. In *Chemistry of Peptides and Proteins*, Vol 4, König WA, Völter W (eds). Attempto Verlag: Tübingen, 1989; 79–86.
24. Enraf-Nonius. *CAD4 Software, version 5.0*. 1989; Enraf-Nonius: Delft, The Netherlands.
25. du Boulay DJ, Hall SR. DIFDAT, ADDREF, SORTRF, ABSOR, GENTAN, CIFIO in Xtal3.7 system, Hall SR, du Boulay DJ, Olthof-Hazekamp R (eds). University of Western Australia, Australia, 2000.
26. Sheldrick GM, Schneider TR. In *Methods in Enzymology* **277**, Sweet RM, Carter CW Jr, (eds). Academic Press: Orlando, FL, 1997; 319–343.
27. Burnett MN, Johnson CK. *ORTEP-III: Oak Ridge Thermal Ellipsoid Plot Program for Crystal Structure Illustrations*. ORNL-6895. Union Carbide Corp.: Oak Ridge National Laboratory, TN, USA, 1996.
28. Davenport G, Hall SR, Dreissig W. *ORTEP in Xtal3.7 System* Hall SR, du Boulay DJ, Olthof-Hazekamp R (eds). University of Western Australia, Australia, 2000.
29. IUPAC-IUB Commission of Biochemical Nomenclature. Abbreviations and symbols for the description of the conformation of polypeptide chains. Tentative rules. *Biochemistry* 1970; **9**: 3471–3479.
30. Richardson JS. The anatomy and taxonomy of protein structure. *Adv. Prot. Chem.* 1981; **34**: 167–339.
31. Baker EN, Hubbard RE. Hydrogen bonding in globular proteins. *Prog. Biophys. Mol. Biol.* 1984; **44**: 97–179.
32. Paterson Y, Rumsey SM, Benedetti E, Némethy G, Scheraga HA. Sensitivity of polypeptide conformation to geometry. Theoretical conformational analysis of oligomers of α-aminoisobutyric acid. *J. Am. Chem. Soc* 1981; **103**: 2947–2955.
33. Geßmann R, Brückner H, Kokkinidis M. The crystal structures of the synthetic *C*-terminal octa- and

dodecapeptides of trichovirin. *J. Pept. Sci.* 1999; **5**: 83–95.
34. Spek AL. *PLATON, A Multipurpose Crystallographic Tool*. Utrecht University, Utrecht, The Netherlands, 2002.
35. SERC Daresbury Laboratory. *CCP4. A Suite of Programs for Protein Crystallography*. SERC Daresbury Laboratory, Warrington, UK, 1979.
36. Humphrey W, Dalke A, Schulten K. VMD — visual molecular dynamics. *J. Mol. Graphics* 1996; **14**: 33–38.
37. Bansal M, Kumar S, Velavan R. HELANAL: a program to characterize helix geometry in proteins. *J. Biomol. Struct. Dyn.* 2000; **17**: 811–819.
38. Marshall GR, Hodgkin EE, Langs DA, Smith GD, Zabrocki J, Leplawy MT. Factors governing helical preference of peptides containing multiple α,α-dialkalyl amino acids. *Proc. Natl Acad. Sci. USA* 1990; **87**: 487–491.
39. Aleman C, Subirana JA, Perez JJ. A molecular mechanical study of the structure of poly(α-aminoisobutyric acid). *Biopolymers* 1992; **32**: 621–631.
40. Karle IL, Flippen-Anderson JL, Sukumar M, Balaram P. Monoclinic polymorph of Boc-Trp-Ile-Ala-Aib-Ile-Val-Aib-Leu-Aib-Pro-OMe (anhydrous). *Int. J. Pept. Protein Res.* 1988; **31**: 567–576.
41. Hodgkin EE, Clark JD, Miller KR, Marshall GR. Conformational analysis and helical preferences of normal and α, α-dialkyl amino acids. *Biopolymers* 1990; **30**: 533–546.
42. Wang Y, Kuczera K. Multidimensional conformational free energy surface exploration: helical states of Ala_n and Aib_n peptides. *J. Phys. Chem. B* 1997; **101**: 5205–5213.
43. Improta R, Barone V, Kudin KN, Scuseria GE. Structure and conformational behavior of biopolymers by density functional calculations employing periodic boundary conditions. I. The case of polyglycine, polyalanine, and poly-α-aminoisobutyric acid *in vacuo*. *J. Am. Chem. Soc.* 2001; **123**: 3311–3322.
44. Zhang L, Hermans J. 3_{10}- helix *versus* α-helix: a molecular dynamics study of conformational preferences of Aib and alanine. *J. Am. Chem. Soc.* 1994; **116**: 11 915–11 921.
45. Smythe ML, Huston SE, Marshall GR. Free energy profile of a 3_{10}- to α-helical transition of an oligopeptide in various solvents. *J. Am. Chem. Soc.* 1993; **115**: 11 594–11 595.
46. Smythe ML, Huston SE, Marshall GR. The molten helix: effects of solvation on the α- to 3_{10}- helical transition. *J. Am. Chem. Soc.* 1995; **117**: 5445–5452.

